Endogenous Protease Activation of ENaC: Effect of Serine Protease Inhibition on ENaC Single Channel Properties

Adedotun Adebamiro,[1] Yi Cheng,[3] John P. Johnson,[2] and Robert J. Bridges[3]

[1]Department of Cell Biology and Physiology, University of Pittsburgh, Pittsburgh, PA 15261
[2]Renal-Electrolyte Division, Department of Medicine, University of Pittsburgh School of Medicine, Pittsburgh, PA 15261
[3]Department of Physiology and Biophysics, Rosalind Franklin University of Medicine and Science, North Chicago, IL 60064

Endogenous serine proteases have been reported to control the reabsorption of Na^+ by kidney- and lung-derived epithelial cells via stimulation of electrogenic Na^+ transport mediated by the epithelial Na^+ channel (ENaC). In this study we investigated the effects of aprotinin on ENaC single channel properties using transepithelial fluctuation analysis in the amphibian kidney epithelium, A6. Aprotinin caused a time- and concentration-dependent inhibition (84 ± 10.5%) in the amiloride-sensitive sodium transport (I_{Na}) with a time constant of 18 min and half maximal inhibition constant of 1 μM. Analysis of amiloride analogue blocker–induced fluctuations in I_{Na} showed linear rate–concentration plots with identical blocker on and off rates in control and aprotinin-inhibited conditions. Verification of open-block kinetics allowed for the use of a pulse protocol method (Helman, S.I., X. Liu, K. Baldwin, B.L. Blazer-Yost, and W.J. Els. 1998. *Am. J. Physiol.* 274:C947–C957) to study the same cells under different conditions as well as the reversibility of the aprotinin effect on single channel properties. Aprotinin caused reversible changes in all three single channel properties but only the change in the number of open channels was consistent with the inhibition of I_{Na}. A 50% decrease in I_{Na} was accompanied by 50% increases in the single channel current and open probability but an 80% decrease in the number of open channels. Washout of aprotinin led to a time-dependent restoration of I_{Na} as well as the single channel properties to the control, pre-aprotinin, values. We conclude that protease regulation of I_{Na} is mediated by changes in the number of open channels in the apical membrane. The increase in the single channel current caused by protease inhibition can be explained by a hyperpolarization of the apical membrane potential as active Na^+ channels are retrieved. The paradoxical increase in channel open probability caused by protease inhibition will require further investigation but does suggest a potential compensatory regulatory mechanism to maintain I_{Na} at some minimal threshold value.

The Journal of General Physiology

INTRODUCTION

Absorption of fluids and electrolytes is a function of many epithelia characterized, in many cases, by electrogenic Na^+ transport where the rate limiting step is apical membrane entry mediated by the epithelial Na^+ channel (ENaC) (Garty and Palmer, 1997). In addition to well-known endocrine regulation of ENaC through intracellular steroid receptors (Garty, 2000) and second messengers such as cAMP (Benos et al., 1996) and Ca^{2+} (Kunzelmann et al., 2001), a new means of regulation by extracellular proteases was recently described (Vallet et al., 1997) and referred to as channel activating protease (CAP) regulation of ENaC. CAP regulation of ENaC may play a role in a variety of physiological functions from blood pressure regulation (Snyder, 2002) to mucocilliary clearance in the airways (Boucher, 2004) and hearing (Rossier, 2004). Three putative CAPs, CAP1 (prostasin), CAP2 (TMPRSS4), and CAP3 (matriptase) that stimulate ENaC-mediated amiloride-sensitive Na^+ transport (I_{Na}) in *Xenopus* oocytes have been cloned (Vuagniaux et al., 2002). These CAPs were predicted to be membrane-anchored proteins with extracellular serine protease domains. The importance of serine protease activity in ENaC regulation has been demonstrated in renal epithelial cell lines (Vallet et al., 1997; Nakhoul et al., 1998; Vuagniaux et al., 2000) and primary airway cells (Bridges et al., 2001; Donaldson et al., 2002) by serine protease inhibition.

Vallet et al. (2002) reported that both membrane anchoring and proteolytic activity were required for CAP1 activation of ENaC. However, the exogenous addition of chymotrypsin and trypsin have also been shown to stimulate I_{Na} in *Xenopus* oocytes (Chraibi et al., 1998), and trypsin stimulates I_{Na} in fibroblasts expressing ENaC (Caldwell et al., 2004). Recently, it was shown that the appearance of apparently smaller molecular weight forms of ENaC from MDCK cells heterologously expressing ENaC could be blocked by mutations that remove putative cleavage sites in ENaC α and γ subunits for the protein convertase furin (Hughey et al., 2004). These mutations were associated

Correspondence to Robert J. Bridges:
bob.bridges@rosalindfranklin.edu

Abbreviations used in this paper: CAP, channel activating protease; CDPC, 6-chloro-3,5-diaminopyrazine carboxamide; ENaC, epithelial Na^+ channel; PAR, protease-activated receptor; PDS, power density spectra.

with a significant decrease of I_{Na} in *Xenopus* oocytes expressing ENaC. Although exogenous proteases have no effect on the spontaneous I_{Na} in several native Na^+ transporting epithelia, trypsin enhanced recovery of I_{Na} following inhibition by the serine protease inhibitors aprotinin and bikunin (Vallet et al., 1997; Bridges et al., 2001; Donaldson et al., 2002). Therefore, inhibition of the CAP pathway by specific protease inhibitors is sufficient to inhibit Na^+ transport in numerous epithelia.

ENaC regulation by the CAP pathway could be mediated by changes in the single channel current (i_{Na}), the open probability (P_o), or the number of active channels (N_T). Studies using ENaC heterologously expressed in oocytes (Chraibi et al., 1998; Adachi et al., 2001) and fibroblasts (Caldwell et al., 2004) have yielded contradictory results in regards to how extracellular proteases regulate ENaC. In an effort to further clarify how ENaC is regulated by the CAP pathway we have used the amphibian renal epithelial cell line A6 and transepithelial current fluctuation analysis. Our results demonstrate that the protease inhibitor aprotinin reversibly inhibits I_{Na}. The decrease in I_{Na} was accompanied by a decrease in the number of open channels (N_o), an increase in i_{Na}, and a paradoxical increase in P_o. Because only the decrease in N_o can explain the decrease in I_{Na} we conclude that the CAP pathway regulates sodium transport by modulating the number of active ENaCs in the apical membrane.

MATERIALS AND METHODS

Cell Culture

A6 cells were maintained in amphibian medium (Biowhitaker) and 10% FBS (GIBCO BRL) in an incubator with humidified air and 4% CO_2 at 28°C as previously described (Rokaw et al., 1996). The cells were expanded on plastic tissue culture dishes and then seeded on Costar Transwell permeable supports (polycarbonate membrane of 0.4 μm pore size and 1 cm^2 area). Experiments were performed 14–21 d after seeding on the permeable supports and 24–48 h after media replacement.

Short-circuit Current (I_{sc}) Measurement

Costar Transwell cell culture inserts were mounted in Costar Ussing chambers and continuously voltage clamped to 0 mV with an automatic voltage clamp (Department of Bioengineering, University of Iowa). Four millivolt bipolar pulses were applied every minute, generating current deflections used to calculate the transepithelial resistance (R_T) with Ohms law. I_{sc} traces were digitized at 10 Hz and recorded using a DASA 6600 acquisition board and Acquire 6600 recording software (Gould Instrument System). The bath solution was identical in the apical and basolateral chambers and contained (in mM) 100 NaCl, 2.4 $KHCO_3$, 1 $CaCl_2$, 5 glucose. The pH of the solution was 8.0 when gassed with ambient air. All experiments were performed at room temperature.

Blocker-induced Fluctuation Analysis

A6 cells on Costar Transwell inserts were placed in Costar Ussing chambers and continuously short circuited with a low noise voltage clamp previously described (Van Driessche and Lindemann, 1978). The I_{sc} was high-pass filtered to remove the DC component and then subjected to anti-aliasing filtering and amplification. The resulting signal was digitized and Fourier transformed to generate power density spectra (PDS) normalized to the tissue surface area (Van Driessche and Lindemann, 1979). PDS were collected at 0.5 Hz fundamental frequency as averages of 30 sweeps over a frequency range of 0.5–350 Hz. The data was then fitted to a Lorentzian noise function $S_0/(1 + (f/f_c)^2)$ plus a "one over f" component defined as $S1/f^{\alpha}$ (Paunescu et al., 2000). "One over f" noise, also called flicker noise, is the excess noise that results from fluctuations in conductance of porous membranes held away from electrical equilibrium that decreases as 1/f (DeFelice, 1981). S1 is the low frequency power of the "one over f" noise with its decay characterized by α ranging from 0.5 to 1.5. We determined the plateau power (S_o) and corner frequency (f_c) from fits of 44 data points in the 0.5–200 Hz range. Blocker-dependent parameters were determined as previously described (Helman and Baxendale, 1990; Els and Helman, 1997; Helman et al., 1998). We determined aprotinin-dependent changes in single channel parameters using two approaches; a cumulative 6-chloro-3,5-diaminopyrazine carboxamide (CDPC) concentration step and a pulse protocol (Helman et al., 1998). CDPC was chosen because its low affinity and high off rate (see below) permit measurements of Lorentzians at relatively uninhibited states and affords a number of experimental advantages. These advantages were well described by Helman and Baxendale (1990). First, low affinity CDPC blockade minimizes the poorly understood "autoregulatory" responses to significant current inhibition that occurs with higher affinity blockers. Second, CDPC permits simultaneous measurement of changes in steady-state current and blocker kinetics from spectral analysis necessary for the determination of the open probability from the three-state model. Third, a low affinity blocker by virtue of a high off rate reduces the relative error in the estimation of the off rate from the linear regression of the corner frequency versus blocker concentration.

The cumulative concentration step approach was performed by mounting A6 cells in a fixed bath volume (5 ml) where 4 μM aprotinin or PBS was added to the apical side. Apical and basolateral solutions were continuously mixed and oxygenated by a gas lift using air. After incubating in 4 μM aprotinin or PBS for 30 min, increasing doses of CDPC (in DMSO) were added to the apical bath to yield a cumulative increase in CDPC concentration. The concentrations used were 10, 20, 30, 40, and 50 μM CDPC. PDS were obtained 2 min after addition of each dose of CDPC and following establishment of a new steady-state I_{sc}. The ENaC-mediated Na^+ current (I_{Na}) was taken as the I_{sc} before minus the I_{sc} remaining after addition of 10 μM amiloride and usually accounted for >90% of the I_{SC}. Blocker rate coefficients were calculated from the linear regression of $2\pi f_c$ vs. blocker concentration using a pseudo-first order kinetic description where $2\pi f_c = k_{off} + k_{on} \cdot [B]$ (k_{on} and k_{off} are the apparent on- and off-coefficients of the blocker (B) interacting with the open channel) and the dissociation constant was calculated as $K_d = k_{off}/k_{on}$. For the pulse protocol, the Ussing chamber was modified to reduce the apical volume to 1.5 ml. The cells were continuously perfused at 5 ml/min with ringer containing 10 μM CDPC. At indicated time points, PDS were obtained, the solution was switched to one with 30 μM CDPC, PDS were again obtained, and then the solution was switched back to one with 10 μM CDPC. Three experimental periods were evaluated: (1) control, 30 min of perfusion without aprotinin; (2) aprotinin, 45 min of perfusion with a solution containing 10 μM aprotinin; and (3) washout, 30 min of perfusion without aprotinin. PDS were obtained at 10 and 30 μM CDPC at 10, 20, and 30 min of the control and washout periods and at 25, 35, and 45 min of the aprotinin period. The blocker rate coefficients were calculated from the two blocker concentrations and corner frequencies as:

$$k_{on} = \frac{2\pi(f_c(30) - f_c(10))}{30 \cdot \mu M - 10 \cdot \mu M},$$

where $f_c(10)$ and $f_c(30)$ are the corner frequencies at 10 and 30 μM CDPC and $k_{off} = 2\pi f_c(10) - k_{on} \cdot 10 \cdot \mu M$. The single channel current amplitude (i_{Na}) was calculated as:

$$i_{Na} = \frac{S_0 \cdot (2\pi f_c(10))^2}{4 \cdot I_{Na}(10) \cdot k_{on} \cdot 10 \cdot \mu M}, \quad (1)$$

where I_{Na} is the amiloride-sensitive current thus allowing us to determine the number of open channels at 10 μM CPDC as $N_o = I_{Na}(10)/i_{Na}$. It has been extensively verified that CDPC and its analogs interact with ENaC-mediated amiloride-sensitive Na^+ transport in a manner described satisfactorily by a three-state model (Lindemann and Van Driessche, 1978; Li and Lindemann, 1983; Abramcheck et al., 1985; Els and Helman, 1989, 1997; Helman and Baxendale, 1990; Els et al., 1991; Baxendale-Cox et al., 1997; Helman et al., 1998; Becchetti et al., 2002). The use of a closed-open blocked three-state model instead of two-state or more complicated four-state models is not the focus of this work and arguments for the use of a three-state model of CDPC blockade of I_{Na} in A6 cells can be found in Helman and Baxendale (1990) and Helman et al. (1998). Therefore, the open probability (P_o) was calculated assuming a three-state model where the blocker interacts with the open state using:

$$P_o = \frac{\left(1 - \frac{I_{Na}(30)}{I_{Na}(10)}\right) \cdot K_d}{30 \cdot \mu M \cdot \frac{I_{Na}(30)}{I_{Na}(10)} - 10 \cdot \mu M}, \quad (2)$$

where $I_{Na}(10)$ and $I_{Na}(30)$ are the amiloride-sensitive current at 10 and 30 μM CDPC (Helman et al., 1998). The number of active channels (N_T) was calculated from

$$N_T = N_o \cdot \left(\frac{1}{P_o} + \frac{10}{K_d}\right). \quad (3)$$

Cell Surface Biotinylation and Western Blot Analysis

Confluent A6 cell monolayers grown on permeable filters (Costar; 75 mm diameter) were treated with PBS, 10 μM aprotinin for 1 h, or 100 nM aldosterone for 6 h and then kept on ice. Cell surface biotinylation and Western blot analysis of ENaC subunits were performed according to the modified method as previously described (Gottardi et al., 1995; Hanwell et al., 2002). In brief, cells were washed three times in ice-cold PBS-CM (PBS with 1 mM $MgCl_2$ and 0.1 mM $CaCl_2$) and incubated with 1.5 mg/ml EZ-link Sulfo-NHS-S-S-biotin (Pierce Chemical Co.) in cold biotinylation buffer (10 mM triethanolamine, 2 mM $CaCl_2$, 150 mM NaCl, pH 9.0) with gentle agitation. Cells were washed once with quenching buffer (192 mM glycine, 25 mM Tris in PBS-CM) and incubated for 20 min with quenching buffer. Cells were then rinsed twice with PBS-CM, scraped in cold PBS, and pelleted at 2,000 rpm at 4°C. The cells were lysed in lysis buffer (1.0% Triton X-100, 150 mM NaCl, 5 mM EDTA, 50 mM Tris) and incubated on ice for 60 min before centrifugation (10 min at 14,000 *g*, 4°C). Supernatants were transferred to new tubes and protein concentration was determined with Coomassie plus protein assay kit (Pierce Chemical Co.). 750 μg of supernatant from each sample was incubated with 100 μl of 50% slurry of streptavidin–agarose beads for 2 h at 4°C. Beads were pelleted by brief centrifugation and then were washed three times with HNTG (20 mM HEPES, pH 7.5, 150 mM NaCl, 0.1% Triton X-100, 10% glycerol). Biotinylated proteins were eluted by boiling in sample buffer supplemented with 5% β-mercaptoethanol. Proteins were separated on 4–20% SDS-PAGE and were transferred to Immobilon-P membranes (Millipore). Proteins were detected by Western blot with polyclonal antibodies against α, β, and γ ENaC subunits. ENaC antibodies were provided by C. Canessa (Yale University School of Medicine, New Haven, CT). The signal was developed with Supersignal west femto maximum sensitivity substrate (Pierce Chemical Co.) and detected with X-Omat Blue XB-1 imaging film (Kodak). Signal intensities were quantified with scanning densitometry (Bio-Rad Laboratories).

Statistical Analysis

Data points represent the mean of *n* individual experiments ± SEM. Statistical comparisons were performed with either unpaired *t* tests when comparing across experiments but paired *t* tests when comparing across conditions in the same cells. The $P < 0.05$ was considered significant. The P values are reported relative to 0.01 and 0.05 in the text and figure legends. Linear regressions were performed with Origin (Microcal). Nonlinear curve fittings were performed with Matlab (Mathworks).

Materials

Unless otherwise stated, all materials were obtained from Sigma-Aldrich.

RESULTS

Effect of Aprotinin on I_{Na}

Apical administration of 10 μM aprotinin resulted in a decrease of I_{sc}. Short circuit current traces of the effects of PBS and aprotinin on A6 cell sodium transport are shown in Fig. 1 (A and B). After a 25–30-min equilibration period following initiation of transepithelial voltage clamping, PBS or aprotinin was added to the apical side for 50 min followed by 10 μM amiloride to obtain a measure of net electrogenic sodium transport mediated by the amiloride-sensitive sodium channel ENaC (I_{Na}). We verified that under these experimental conditions >90% of the I_{SC} was amiloride sensitive (unpublished data). Thus any change in the I_{SC} can be attributed to a change in I_{Na}. The I_{sc} taken after the equilibration period is referred to as the control I_{sc}. As can be seen, aprotinin caused a time-dependent decrease in the I_{SC} that was not observed in the PBS (vehicle control) treated cells. The decrease in I_{sc} caused by aprotinin was apparent following a variable short lag phase of ~30 s. In this subset of experiments, the PBS-treated monolayers had a control I_{sc} of 8.4 ± 1.36 μA/cm² ($n = 12$) that was not significantly changed (8.9 ± 1.08 μA/cm², $P > 0.05$) 50 min after addition of PBS but was reduced to 0.8 ± 0.13 μA/cm² upon addition of 10 μM amiloride. Parallel experiments with 10 μM aprotinin added to the apical side had control I_{sc} of 7.5 ± 1.25 μA/cm² ($n = 12$) that was reduced to 2.2 ± 0.55 μA/cm² ($P < 0.01$) 50 min after addition of aprotinin and further reduced to 0.5 ± 0.12 μA/cm² with the addition of 10 μM amiloride. Thus I_{Na} was reduced from 8.1 ± 1.1 μA/cm² in the PBS-treated cells to 1.7 ± 0.53 μA/cm² in the aprotinin-treated cells. These results are summarized in Fig. 1 C.

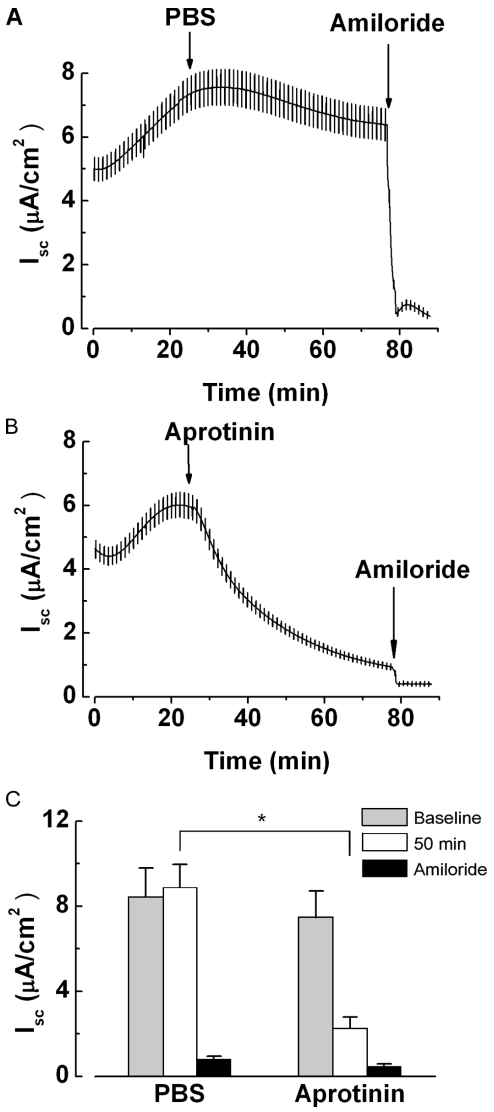

Figure 1. Effect of apically administered aprotinin on amiloride-sensitive I_{SC} in A6 cell monolayers. A6 cells in Ussing chambers with symmetrical bath solutions continuously gassed with air were voltage clamped at 0 mV and I_{SC} monitored. After a 25–30-min equilibration period (A) PBS or (B) aprotinin 10 μM was added to the apical bath. I_{SC} was monitored for 50 min then 10 μM amiloride was added to the apical bath to determine I_{Na}. The current deflections are responses to 4 mV bipolar pulses used to measure transepithelial resistance. (C) The mean values of I_{SC} before (shaded bar), 50 min after addition of PBS/aprotinin (hatched bars), and following addition of amiloride (filled bars) indicate substantial decrease of I_{SC} by aprotinin. The error bars are ± SEM. Significant decrease was found in comparing I_{SC} values before and 50 min following addition of aprotinin but not PBS with $n = 12$ and 14 filters for PBS and aprotinin experiments, respectively (*, $P < 0.01$).

The inhibition of I_{Na} by aprotinin was time dependent. The decrease in I_{Na} as a percentage of control I_{Na} following addition of 10 μM aprotinin was fitted to an exponential decay (% control = a*exp(−t/τ) + b) as illustrated in Fig. 2 A. Using the period starting 5 min and ending 45 min after addition of aprotinin, τ was 18 ± 1.2 min. Aprotinin (10 μM) inhibited 84 ± 10.5% of the control I_{Na} in this subset of filters. The effect of aprotinin on I_{Na} was also concentration dependent (Fig. 2 B). The half-maximal inhibition constant ($K_{1/2}$), determined by fitting the I_{Na} as a percentage of control I_{Na} versus aprotinin concentration to a simple inhibition curve (% control = a*$K_{1/2}$/($K_{1/2}$ + [aprotinin]) + b; see Fig. 2 legend), was 1.0 ± 0.13 μM, with a maximal inhibition of 80 ± 12%. The kinetic fits suggest a high-affinity inhibition of the majority of the I_{Na} by aprotinin. R_T was maintained after addition of 10 μM aprotinin. The decrease in I_{Na} caused by aprotinin was accompanied by a tendency toward increasing R_T particularly in filters that had relatively high control I_{Na}. The R_T before addition of PBS and aprotinin was 5.15 ± 0.46 and 4.90 ± 0.57 kΩcm² respectively. Following the addition of PBS and aprotinin for 50 min the R_T was 4.6 ± 0.46 and 6.1 ± 0.53 kΩcm², respectively, thus the integrity of the epithelial monolayer was not compromised by aprotinin incubation.

Effect of Aprotinin on Blocking of ENaC by the Amiloride Analogue CDPC

The blockade of I_{Na} by CDPC for PBS and aprotinin-treated A6 was first measured by a cumulative concentration response determination using a step protocol. PBS or 4 μM aprotinin was introduced to the apical side of the A6 filters for 30 min before commencing the CDPC concentration step protocol, which was performed over 30 min. The concentration of 4 μM aprotinin was used because this concentration was capable of significantly inhibiting I_{Na} but sufficient current remains at the higher CDPC blocker concentrations to ensure adequate measurement of the Lorentzian component in the PDS. As shown in Fig. 3 A, PBS-treated cells had significantly higher I_{Na} (6.1 ± 0.40 μA/cm²) compared with aprotinin-treated cells (2.8 ± 0.59 μA/cm², $P < 0.01$) at 0 μM CDPC and also at all other concentrations studied (10, 20, 30, 40, and 50 μM). CDPC caused a concentration-dependent decrease in I_{Na} in both PBS- and aprotinin-treated A6 cells, thus the sensitivity to blockade of I_{Na} by CDPC was maintained in the presence of aprotinin. The PDS in both PBS- and aprotinin-treated A6 had Lorentzian components that varied with CDPC concentration (Fig. 4, A and B). As expected from a smaller I_{Na}, the Lorentzian S_o values were also significantly decreased in aprotinin-treated cells ($P < 0.01$) at the blocker concentrations studied. The S_o values remained biphasic with respect to blocker concentration in both the PBS and aprotinin studies. The data were fitted to the equation describing the S_o of a two-state kinetic scheme and a biphasic curve was obtained. The S_o maxima were at 18.7 ± 0.28 μM and 15.5 ± 0.71 μM CDPC for PBS- and aprotinin-treated

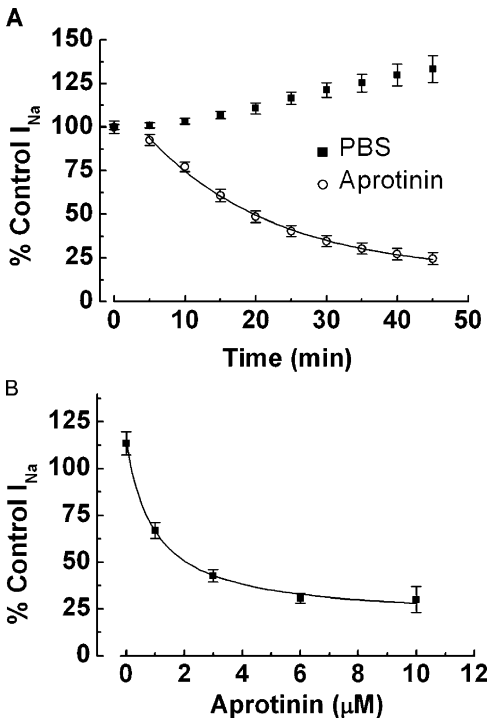

Figure 2. Time and concentration dependence of the effect of aprotinin on I_{Na}. (A) I_{Na} after apical administration of PBS (filled squares) or 10 μM aprotinin (open circles) was plotted as a percentage of I_{Na} before administration (control) using data recorded at 5-min intervals. The data points plotted represent the mean values of 12 filters each for PBS and aprotinin addition with error bars corresponding to ± SEM. A small time-dependent increase in I_{Na} could be seen with PBS addition but was not consistently observed in all the filters measured. The solid line through the aprotinin data points represents a fit to an exponential decay % control I_{Na} = a*exp(−t/τ) + b ignoring the time = 0 data point. The constants a and b represent the percentage of I_{Na} sensitive and insensitive to 10 μM aprotinin, respectively. The mean control I_{Na} for the set of 24 filters used in this experiment was 8.2 ± 0.36 μA/cm^2. (B) The % control I_{Na} was measured at 50 min after adding the indicated concentration 0, 1, 3, 6, 10 μM of aprotinin (filled squares) and demonstrated a concentration dependence to the aprotinin inhibition of I_{Na}. The solid line represents a fit to the inhibition curve % control = a*$K_{1/2}$/$K_{1/2}$ + [aprotinin] + b, where $K_{1/2}$ is an inhibition constant; a and b represent the aprotinin sensitive and insensitive percentages of I_{Na}, respectively. The mean control I_{Na} for the set of 25 filters used in this experiment was 4.1 ± 0.30 μA/cm^2. Error bars are ± SEM.

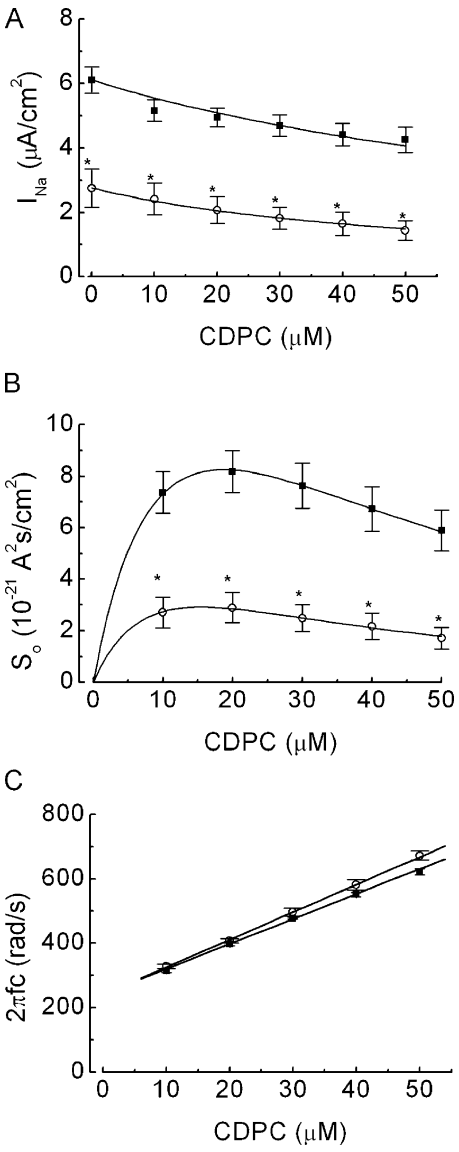

Figure 3. Aprotinin effect on blocker-induced fluctuation of I_{Na} in A6 cells. A6 cells in Ussing chambers were continuously voltage clamped at 0 mV and the I_{SC} monitored on a strip chart for 30 min following addition of PBS (filled squares) or aprotinin 4 μM (open circles). Cumulative step increases in the concentration of CDPC in the apical bath were performed, the I_{SC} and power density spectra were obtained at each blocker concentration 10, 20, 30, 40, and 50 μM. The values are given as the mean (n = 8 for PBS and n = 6 for aprotinin-treated A6 filters) ± SEM. (A) The I_{Na} following 30 min of PBS addition was significantly higher than I_{Na} following aprotinin addition (*, P < 0.01). In both conditions CDPC decreased the I_{Na} and the decrease could be explained by simple Michaelis-Menten inhibition kinetics (solid lines). (B) The S_o at increasing concentration of CDPC was biphasic and was fitted to a two-state channel blocking model (solid lines) in both cases. The difference in magnitude of S_o between PBS and aprotinin-treated A6 cells was significant (*, P < 0.01). (C) $2\pi f_c$ plots with linear regressions (solid lines) from which k_{on} and k_{off} were calculated were virtually identical for PBS and aprotinin-treated cells.

A6, respectively (Fig. 3 B). Since the maximum value of S_0 occurs at the blocker concentration of $0.5k_{off}/k_{on}$, the lack of a change in the blocker concentration at maximum S_0 in the absence or presence of aprotinin showed that the ratio k_{off}/k_{on} and hence the dissociation constant of the blocker was unaltered. The second indication came from measurement of the $2\pi f_c$ values at the CDPC concentrations used. For both PBS- and aprotinin-treated A6 cells, the $2\pi f_c$ increased linearly with respect to blocker concentration. A linear regression of the data demonstrated that the apparent rate

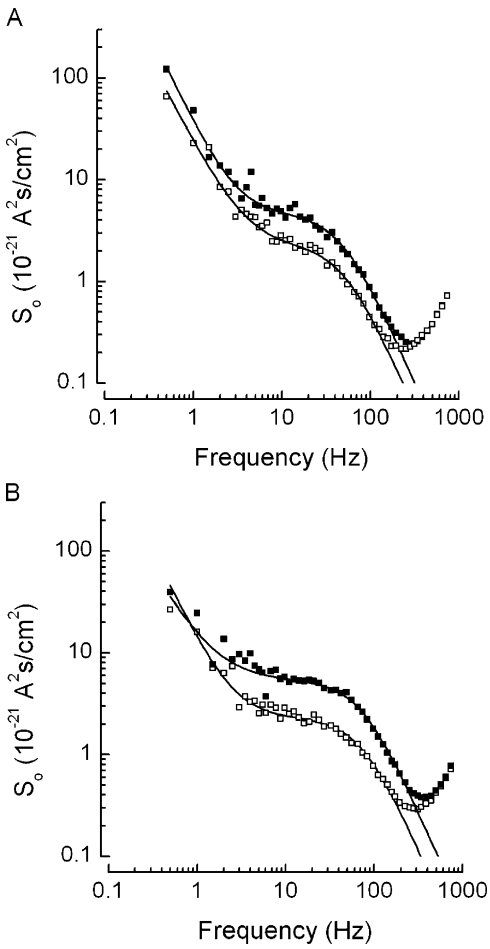

Figure 4. Typical current noise power spectral density in the absence (solid squares; 3.87 μA/cm² I_{Na}) and presence (open squares; 1.67 μA/cm² I_{Na}) of aprotinin are shown at 10 μM CDPC (A) and 30 μM CDPC (B). Corner frequencies were 47.6 and 50.2 Hz (A) (at 10 μM CDPC) in and 72.4 and 72.7 Hz (B) (at 30 μM CDPC) in the absence and presence of aprotinin, respectively. The solid lines represents the fit of the data to the sum of Lorentzian plus low frequency "1/f" noise.

coefficients were not different (Fig. 3 C). The k_{off} and k_{on} were 242 ± 5.40 s^{-1} and 7.8 ± 0.19 $\mu M^{-1}s^{-1}$ for PBS experiments (n = 8). These constants were not significantly different in aprotinin experiments (n = 6) at 240 ± 3.78 s^{-1} and 8.6 ± 0.15 $\mu M^{-1}s^{-1}$, respectively ($P > 0.05$). The blocker dissociation constant K_d was 31.2 and 28.1 μM CDPC for PBS- and aprotinin-treated A6 cells, respectively. The biphasic dependence of S_o on blocker concentration and the linear dependence of $2\pi f_c$ on blocker concentration indicated a simple pseudo first order blocker–ENaC binding in PBS- and aprotinin-treated A6. Consequently, only two concentration points were required to determine the blocking kinetics as well as the single channel parameters as previously described (Helman et al., 1998). To avoid autoregulatory responses of I_{Na} to prolonged blocker-induced decreases in I_{Na} caused by cumulative increases in blocker concentration (Abramcheck et al., 1985; Tang et al., 1985; Els et al., 1991), a pulse-protocol approach was employed to measure the single channel properties.

Single Channel Properties: CDPC Pulse Protocol

To avoid blocker-induced autoregulation of ENaC and to study the single channel properties of the same cells in control and aprotinin-treated periods as well as measure reversibility of the aprotinin effect, a pulse protocol approach was employed pulsing between 10 and 30 μM CDPC (Helman et al., 1998). Typical PDS in control and aprotinin-treated periods at 10 and 30 μM CDPC are shown in Fig. 4. The two CDPC concentrations were chosen because they were close to the S_o maxima as shown in the step protocol experiments (Fig. 3 B), thus providing the highest signal for the Lorentzian component in the PDS while producing measurable changes in I_{Na} and significant changes in $2\pi f_c$. Secondarily, 10 and 30 μM CDPC could be used in both the control and aprotinin periods because the blocker kinetics were identical in the absence and presence of aprotinin. The I_{Na}, i_{Na}, P_o, and N_o were measured before (control), while perfusing with aprotinin (aprotinin), and following removal of aprotinin from the apical side (washout) in eight filters as illustrated in Fig. 5. The I_{Na} was 3.4 ± 0.17 μA/cm² under control conditions and was reduced to 1.4 ± 0.17 μA/cm² 35 min after addition of 10 μM aprotinin ($P < 0.01$). Following washout of aprotinin, I_{Na} recovered to control levels (3.2 ± 0.11 μA/cm²). The recovery appears to be complete by 10 min after washout as subsequent time points did not show further increases in I_{Na}. The i_{Na} was 0.46 ± 0.037 pA in the control period, increased to 0.70 ± 0.069 pA ($P < 0.05$) 35 min after addition of aprotinin, and returned to 0.45 ± 0.018 pA following removal of aprotinin. The P_o was 0.23 ± 0.031 before aprotinin addition, approached a maximum of 0.41 ± 0.075 ($P < 0.05$) 15 min after aprotinin addition, and then returned to 0.23 ± 0.019 after removal of aprotinin. The changes in N_o paralleled changes in I_{Na} with N_o of 8.03 ± 0.812 before, 2.26 ± 0.523 ($P < 0.01$) after aprotinin addition, and 7.21 ± 0.445 million channels/cm² following washout of aprotinin. Since changes in I_{Na} cannot be explained by changes in i_{Na} or P_o, these changes must result from changes in N_T as shown in Fig. 6. N_T was 42 ± 8.24 million channels/cm² before aprotinin addition. N_T was reduced to 8.93 ± 3.351 million channels/cm² after addition of aprotinin and returned to 34.4 ± 5.418 million channels/cm² following aprotinin washout.

Relationship between Single Channel Properties and I_{Na}

To examine how the single channel properties change with I_{Na} we quantified their relationship to I_{Na} by lin-

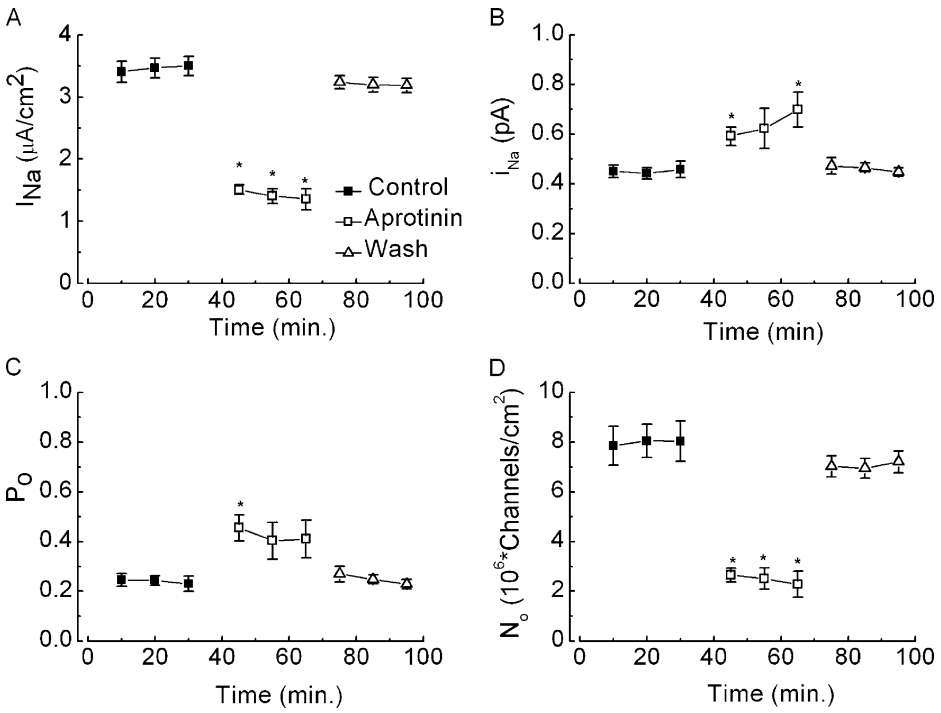

Figure 5. Summary of the changes in the single channel parameters with aprotinin addition and reversal. (A) Summary of reduction in I_{Na} by aprotinin in the pulse protocol experiments. I_{Na} of cells continuously perfused with a ringer solution containing 10 μM CDPC was measured at 10-min intervals before addition of aprotinin (filled squares), then the cells were perfused with 10 μM aprotinin and I_{Na} measured at the indicated times (open squares) after which aprotinin was washed out (open triangles). At 10-min intervals, the CDPC concentration was pulsed to 30 μM and returned to 10 μM for analysis of blocker-induced fluctuations. (B) Summary of changes in i_{Na} following perfusion of aprotinin and washout. The increase in i_{Na} caused by aprotinin was significant (*, $P < 0.01$) and reversible. (C) Summary of changes in P_o. The changes in P_o were significant (*, $P < 0.01$) at 15 min after perfusing with aprotinin and returned to the pre-aprotinin control values following washout of aprotinin. (D) Summary of changes in N_o following aprotinin perfusion showed a significant decrease in N_o (*, $P < 0.01$) that was completely reversed upon removal of aprotinin. Values are reported as mean ± SEM for $n = 8$.

ear regression analysis using the experimental dataset shown in Fig. 5. Because of the apparent differences in the relationship of the single channel properties to I_{Na} in the control, aprotinin, and washout conditions we determined the regressions using data points in each condition. The linear parameters are summarized in Table I. The values of i_{Na} versus I_{Na} in the control and aprotinin-treated conditions are plotted in Fig. 7 A. Over the range of control I_{Na} (2.78–4.17 μA/cm^2), i_{Na} decreased with increases of I_{Na} ($r = -0.62$). The i_{Na} also decreased with increases of I_{Na} ($r = -0.80$) over the aprotinin I_{Na} range (0.87–2.08 μA/cm^2). However, the slope was approximately threefold steeper and the intercept ~50% higher during the aprotinin treatment period compared with the control period. No correlation was observed between i_{Na} and I_{Na} during the wash condition ($r = 0.02$). Plotted also are the P_o values versus I_{Na} in the control and aprotinin-treated conditions (Fig. 7 B). The P_o also decreased with increases of I_{Na} ($r = -0.46$) in the control condition as well as in the presence of aprotinin ($r = -0.75$). In the presence of aprotinin, the slope was approximately fourfold steeper and the intercept increased by ~100%. No correlation was observed between P_o and I_{Na} in the wash condition ($r = -0.17$). We also plotted the N_o versus I_{Na} in the control and aprotinin-treated conditions (Fig. 7 C). We found that N_o increased with increases of I_{Na} in the control condition ($r = 0.86$). This positive correlation remained in the aprotinin ($r = 0.92$) and wash conditions ($r = 0.61$) so that transport is determined primarily by changes of N_o in each condition studied.

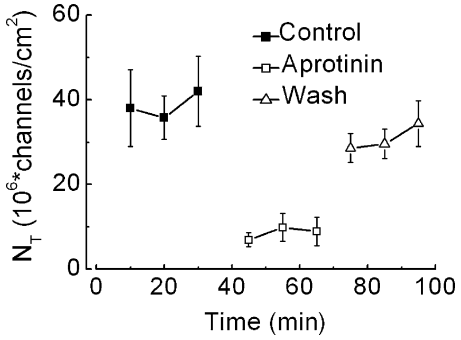

Figure 6. N_T calculated from the P_o and K_d decreased by ~80% following 35 min of inhibition by aprotinin (open squares) compared with control conditions (solid squares). Inhibition of N_T was reversed following washout of aprotinin (open triangles) and returned to control values within 30 min of washout.

Cell Surface Expression

The above results indicate that aprotinin alters the number of active channels in the apical membrane. To determine if this effect is also reflected in changes in ENaC apical membrane protein levels we performed cell surface protein biotinylation studies. We biotinylated apical membrane proteins of A6 cells grown on permeable supports (75 mm diameter). Biotinylated proteins were recovered with streptavidin–agarose beads

TABLE I

Dependence of the Single Channel Properties on the ENaC-mediated Na^+ Current (I_{Na}) in Control, Aprotinin-treated, and Wash Conditions

	i_{Na}			P_o			N_o		
Condition	*r*	Intercept	Slope	r	Intercept	Slope	r	Intercept	Slope
		pA	*pA/(μA/cm²)*			*(μA/cm²)⁻¹*		*10⁶/cm²*	*10⁶/μA*
Control	−0.62	0.82	−0.11	−0.46	0.49	−0.07	0.86	−5.86	4.01
		[0.61, 1.03]	[−0.17, −0.05]		[0.27, 0.71]	[−0.14, −0.01]		[−9.56, −2.17]	[2.95, 5.07]
+Aprotinin	−0.80	1.23	−0.42	−0.75	0.99	−0.40	0.92	−1.84	3.04
		[1.03, 1.43]	[−0.55, −0.28]		[0.76, 1.22]	[−0.55, −0.24]		[−2.66, −1.03]	[2.49, 3.60]
Wash	0.02[a]	0.45	0.00	−0.17[a]	0.35	−0.04	0.61	−0.24	2.28
		[0.14, 0.75]	[−0.09, 0.10]		[0.07, 0.66]	[−0.13, 0.06]		[−4.43, 3.96]	[0.973, 3.58]

r is the regression coefficient. "Intercept" and "Slope" are the linear parameters of the regression. Brackets indicate the lower and upper bounds of the 95% confidence interval of the estimated linear parameters. The regressions are statistically significant ($P < 0.001$) except where stated otherwise.

[a]The regression is not statistically significant ($P > 0.025$).

and we determined subunit density by Western blotting using specific antibodies to each of the ENaC subunits α, β, γ as described by Alvarez de la Rosa et al. (2002, 2004), Gottardi et al. (1995), and Hanwell et al. (2002). Western blots were examined from A6 cells treated with PBS or 10 μM aprotinin for 1 h, or cells treated with 100 nM aldosterone for 6 h. There were two immunoreactive bands for the α subunit at 85 and 65 kD, two for the β subunit at 115 and 100 kD, while one predominant band at 90 kD was observed for the γ subunit. As shown in Fig. 8, quantification of the relative changes in apical membrane subunits indicated that aldosterone increased subunit density two to fourfold as previously reported by Alvarez de la Rosa et al. (2002). In contrast, aprotinin had no detectable effect on the cell surface density of any of the three ENaC subunits. The results summarized in Fig. 8 represent three independent experiments. Alvarez de la Rosa et al. (2002) reported that aldosterone increased cell surface expression of ENaC subunits proportional to an observed increase in I_{SC}. These results confirm that it is possible by biochemical methods to detect changes in N_T and thereby I_{Na} when A6 cells are stimulated with aldosterone. In contrast, the large decreases in N_T in the presence of aprotinin did not correlate with a biochemically detectable decrease in cell surface subunit density.

DISCUSSION

Aprotinin is a 6.5-kD protein that is a potent and reversible Kunitz type inhibitor of several serine proteases including trypsin, plasmin, and kallikreins (Vogel and Werle, 1970). The inhibition of Na^+ transport by apical administration of aprotinin has been reported in toad urinary bladder (Orce et al., 1980), the A6 cell line (Vallet et al., 1997), the mouse cortical collecting duct cell mpkCCD14 cell line (Liu et al., 2002), human bronchial epithelial cells (Bridges et al., 2001; Donaldson et al., 2002), and rat and mouse lung alveolar epithelial cells (Planes et al., 2005). In all cases, aprotinin inhibition of I_{Na} was much slower than the effect caused by the ENaC blocker amiloride. Direct inhibitors of ENaC such as extracellular cations (Chraibi and Horisberger, 2002; Caci et al., 2003) and covalent modification of thiol groups (Snyder, 2000; Snyder et al., 2000) typically demonstrate a rapid time course. Also, evidence of blockade in the form of aprotinin-induced Lorentzians in the PDS or apparent changes in the CDPC-induced Lorentzian that may result from aprotinin competitive inhibition of ENaC (Li et al., 1982) were absent. Inhibition of I_{Na} by aprotinin was evident within 10 min of addition and approached a nonzero nadir with time. The inhibition was characterized by a time constant of ~18 min. The plateau level of inhibition was concentration dependent with high affinity and a maximum inhibition of 70–80%. The micromolar affinity reported here is consistent with measurements performed on the urinary toad bladder (Orce et al., 1980). The concentration dependence and time course suggests that aprotinin inhibits a specific protease-dependent pathway that regulates a large fraction of the epithelial Na^+ transport. The identity of this regulatory protease(s) is a matter of some conjecture.

Kallikrein-like protease activity has been identified at the apical surface and in the apical medium of A6 cells forming a tight monolayer as well as from toad urinary bladder (Jovov et al., 1990). The kallikrein-like protease activity was inhibited by aprotinin at a concentration that inhibited Na^+ transport in A6 cells and toad bladder (Margolius and Chao, 1980). Further, exogenous addition of trypsin and chymotrypsin have been shown to activate I_{Na} in epithelia pretreated with protease inhibitors and activate Na^+-mediated currents in *Xenopus* oocytes expressing ENaC (Vallet et al., 1997; Bridges et al., 2001; Donaldson et al., 2002; Liu et al., 2002). Vallet et al. (1997), using expression cloning methods, identified a channel activating protease (CAP) from A6 cells that increased ENaC-mediated I_{Na}

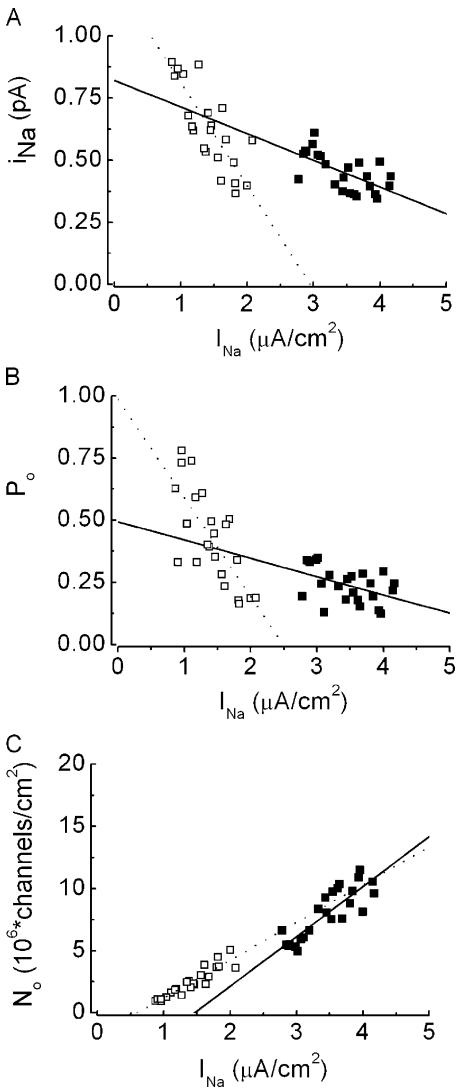

Figure 7. Relationship of single channel parameters to I_{Na}. Individual values of (A) i_{Na}, (B) P_o, and (C) N_o under control conditions (filled squares) and during aprotinin treatment (open squares) plotted against I_{Na}. The data points from the wash conditions have been omitted for clarity. The lines are linear regressions to the control period data (solid line) and aprotinin period data (dotted line). The regressions for all three periods are summarized in Table I.

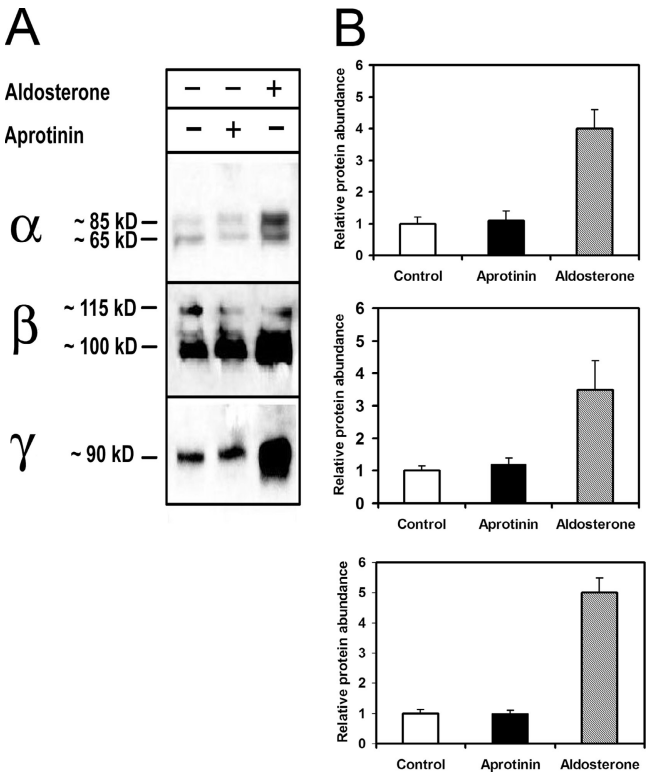

Figure 8. The effect of aprotinin and aldosterone on the relative abundance of ENaC subunits in the apical membrane of A6 cells. (A) A6 cells grown on permeable supports were treated either with PBS or 10 μM aprotinin for 1 h or 100 nM aldosterone for 6 h. Apical proteins were biotinylated and recovered with streptavidin–agarose beads. The recovered proteins were analyzed with antibodies against α, β, and γ *Xenopus* ENaC subunits. Representative Western blots are shown with the arrows indicating the migration of molecular mass standards. (B) Mean of relative changes in apical membrane abundance measured by scanning densitometry and normalized to the control density. The bars represent three independent experiments with error bars corresponding to ±SEM.

in *Xenopus* oocytes. The mammalian homologue of xCAP1 is prostasin/hCAP1 and coexpression of prostatin with ENaC also increases Na^+-mediated currents (Vuagniaux et al., 2000; Adachi et al., 2001). Similar to the secretion of kallikrein-like proteases by amphibian renal cells, prostasin has been found to be secreted in an aldosterone-regulated manner in rat urine (Narikiyo et al., 2002). Bikunin, a Kunitz type serine protease inhibitor with two Kunitz domains, has a submicromolar potency for inhibiting Na^+ transport in human bronchial epithelia (Bridges et al., 2001) and this correlates with the nanomolar inhibition constant reported for aprotinin inhibition of prostasin enzymatic activity in vitro (Shipway et al., 2004). These findings support the idea that prostasin and CAP1 are endogenous proteases that can regulate epithelial Na^+ transport. Consistent with this view is that RNA silencing of CAP1 was sufficient to inhibit I_{Na} in the CF15 airway epithelial cell line to the extent observed with aprotinin on A6 and HBE cells (Tong et al., 2004). Expression cloning has identified two other such CAPs in mammalian renal cells that are capable of stimulating current in *Xenopus* oocytes coexpressing ENaC in an aprotinin-sensitive manner (Vuagniaux et al., 2002). Another possible protease that may regulate Na^+ transport is the ubiquitous convertase furin, which modulated ENaC-mediated currents in the Chinese hamster ovary expression system (Hughey et al., 2004). However furin is not inhibited by aprotinin; consequently, the aprotinin inhibition of I_{Na} cannot be attributed to a furin pathway

of channel activation in A6 cells and human bronchial epithelia. The relative importance of the individual proteases and the mechanism of their action in regulating Na^+ transport are yet to be determined. The studies reported here were designed to investigate the mechanism of action of aprotinin inhibition of epithelial Na^+ transport and thereby how aprotinin-sensitive proteases regulate Na^+ transport.

Single Channel Properties

Na^+ transport is a function of the single channel properties and can be expressed as $I_{Na} = N_T*P_o*i_{Na}$. Using noise analysis we studied the apical Na^+ channels in the presence and absence of aprotinin and found that the decrease in I_{Na} caused by aprotinin can be explained by a decrease in the number of open channels (N_o) and these effects of aprotinin were fully reversible upon aprotinin washout. In contrast, aprotinin caused both i_{Na} and P_o to increase, and thus these changes cannot account for the decrease in I_{Na}. The i_{Na} averaged 0.45 pA under control conditions in the present study, which is similar to previously reported values in short-circuited A6 cells by noise analysis (Helman et al., 1998; Alvarez de la Rosa et al., 2004). Given the i_{Na} of 0.45 pA under control conditions and a single channel conductance of 4–6 pS for the highly selective Na^+ channel in A6 cells (Palmer, 1992; Puoti et al., 1995), a driving force of ~90 mV can be estimated for apical Na^+ entry. A 90-mV effective electromotive force for Na^+ movement across the apical membrane has been reported in A6 cell monolayers with resistances and I_{Na} in the range that we have measured (Granitzer et al., 1991). The average i_{Na} presented here is therefore consistent with the characteristic driving forces across the apical membrane of A6 cell monolayers and the conductance of sodium channels. Application of aprotinin to the apical bath caused a significant increase in i_{Na}. Therefore, the inhibition of I_{Na} by aprotinin cannot be explained by changes in i_{Na}. By definition, $N_o = N_T*P_o$, where N_T is the number of electrically detectable or active channels gating between the open and closed states. A decrease in N_o may arise from a decrease in N_T or a decrease in P_o of the active channels. The P_o of active channels at the apical membrane was measured and in the control condition averaged 0.2. This value of P_o is well within the range that has been measured by noise analysis and patch clamping for ENaC (Helman and Kizer, 1990). With application of aprotinin, the P_o doubled. The increase in P_o would be expected to increase N_o and I_{Na}; however, aprotinin causes a reduction in N_o and I_{Na}. Therefore, aprotinin inhibition of I_{Na} is explained by a decrease in N_T (Fig. 5).

To further elucidate the relationship between I_{Na} and the single channel properties we examined the individual data points from our pulse-protocol experiments. Considering the control conditions, we found a weak negative correlation between i_{Na} and I_{Na}. A negative correlation is expected because increased Na^+ transport rates depolarize the cells, reducing the electromotive force across the Na^+ channels (Granitzer et al., 1992; Blazer-Yost and Helman, 1997). The strength of the correlation is expected to be weak because the driving force across the apical membrane is variable due in part to a high variation in the basolateral resistance from one monolayer to another (Granitzer et al., 1991). Following apical administration of aprotinin, the negative correlation between i and I_{Na} became stronger. Such a correlation cannot explain the decrease in I_{Na}. It however suggests that the effect on i_{Na} is not simply due to the presence of aprotinin but follows the amount of inhibition of I_{Na} caused by the presence of aprotinin. It was found that a negative correlation occurs between the ratio $I_{Na}^{control}/I_{Na}^{aprotinin}$ and $i_{Na}^{control}/i_{Na}^{aprotinin}$, thereby confirming that inhibition of I_{Na} by aprotinin produces the steep inverse relationship seen in the presence of aprotinin. In a similar manner, the P_o from cells under control conditions showed significant variation but a weak negative correlation was evident. This increasing P_o with decreasing I_{Na} may be related to a previously reported hyperpolarization-induced increase in ENaC P_o (Palmer and Frindt, 1988, 1996). As observed in the case of i_{Na}, with aprotinin treatment, the negative correlation between P_o and I_{Na} was intensified, supporting the notion that the P_o change accompanies the decreasing I_{Na} and is not simply due to the presence of aprotinin. For N_o, we found a strong positive correlation with I_{Na} both in the control condition and the in the presence of aprotinin. Since the apical conductance has been shown to be strongly positively correlated with I_{Na} in A6 cells (Granitzer et al., 1991; Helman and Liu, 1997) and the apical conductance is in large part given by the product of N_o and the single channel conductance, it is expected that under control conditions N_o would have a positive correlation with I_{Na}. This correlation persists following treatment with aprotinin. The decrease in I_{Na} following aprotinin treatment is only explained by a decrease in N_o that results from a decrease in N_T.

Mechanism of Inhibition of N_T by Aprotinin

Out of several possible explanations for the decrease in N_T caused by aprotinin, an intriguing explanation is that at the apical membrane there is a turnover of active channels into inactive channels in the presence of aprotinin. The inactive channels can be considered to be "capped" while the active channels are "uncapped." Because multiple proteases have been shown to increase ENaC activity in a variety of systems in a manner dependent on their proteolytic activity, it is possible that ENaC is the substrate for proteolytic uncapping.

Alternatively, ENaC uncapping may occur through proteolysis of a closely associated ENaC regulatory protein, proteolytic generation of a stimulatory ligand, protein–protein interactions of ENaC extracellular domain and the protease, or through generation of intracellular second messengers. Activation of the trypsin receptor protease-activated receptor 2 (PAR2) does not stimulate ENaC (Danahay et al., 2001) and ENaC activation is independent of PAR2 (Chraibi et al., 1998). Furthermore, ENaC activation by serine proteases is independent of G protein–coupled receptors in oocytes (Chraibi et al., 1998) and fibroblasts (Caldwell et al., 2004), yet to date all known PARs are G protein–coupled receptors. There is no finding to support an intracellular second messenger requirement for the protease-mediated uncapping of ENaC. Protein–protein interactions in the extracytoplasmic domain between the protease dipeptidyl aminopeptidase-like protein, DPPX, and neuronal A-type K^+ channels has been implicated in the redistribution of the neuronal channels from the ER to the plasma membrane as well as in the regulation of channel gating (Nadal et al., 2003). The function of DPPX is not associated with proteolytic activity; however it remains to be determined that the protease-like domain is required for DPPX channel-regulating activity. It is difficult to imagine that apically administered aprotinin is rapidly trafficked to the ER where it disrupts a possible DPPX-like interaction of ENaC with a serine protease or that once disrupted, reconstitution and trafficking occur on the time scale observed with exogenous protease reactivation of aprotinin inhibited I_{Na} in epithelia cells. Trafficking from a compartment closer to the apical membrane or direct activation by the protein–protein interaction may cause the uncapping event. If aprotinin inhibits a protease-dependent trafficking of ENaC to the apical membrane from intracellular pools, then the physical channel density is expected to decrease. The quantitation of apical membrane ENaC subunits by cell surface biotinylation, however, shows that the steady-state densities of α, β, and γ subunits were unchanged in the presence of aprotinin. Thus it appears unlikely that aprotinin mediates ENaC trafficking to alter steady-state sodium current in A6 cells. Recent investigations suggest that the biochemically detected apical membrane protein subunit density may be one to two orders of magnitude greater than electrically detectable channels (Alvarez de la Rosa et al., 2004). Although the aldosterone-mediated changes in subunit density and I_{SC} are detectable, a similar correlation could not be detected for the aprotinin-mediated changes in I_{Na}. These results may mean aprotinin does not alter cell surface expression of ENaC subunit or that any changes are beyond the resolution of present biochemical methods. The high level of subunit protein at the apical surface would also impair the detection of proteolytically cleaved ENaC subunits.

There is, however, some evidence to support the idea that uncapping may occur through proteolysis of ENaC. A low apparent molecular weight form of the γ subunit immunoreactive band on Western blots was induced by aldosterone (Masilamani et al., 1999). The new size was consistent with excision of an amino-terminal region immediately after the first transmembrane domain. Aldosterone up-regulation of CAP1 (Narikiyo et al., 2002) and subsequent ENaC cleavage may explain the observations by Masilamani et al. (1999). Molecular weight reductions attributable to proteolytic cleavages in α and γ subunits in MDCK cells expressing ENaC were recently reported and found critical for channel activity (Hughey et al., 2003, 2004). In A6 cells, a fast and slow migrating α ENaC immunoreactive band has been reported with the fast form seen primarily at the apical membrane (Alvarez de la Rosa et al., 2002). However, this fast migrating band form appears to result from the formation of stable disulfide bonds following maturation. Although extensive processing of ENaC resulting in the change of the apparent molecular weight of its subunits have been observed, the data remains inconclusive as to whether ENaC is proteolytically cleaved in A6 cells and whether the cleavage results in the phenomenon we term uncapping. Independent of the mechanism, protease-mediated uncapping was apparently irreversible in oocyte studies, suggesting that channels cannot be recapped (Chraibi et al., 1998).

A simple hypothesis that explains aprotinin inhibition of I_{Na} is that endocytosis of uncapped channels (i.e., active channels) is responsible for the loss of current in the presence of aprotinin, as aprotinin prevents the uncapping of capped channels (i.e., inactive channels) newly inserted into the apical membrane. The half-life (11–17 min) measured for the α, β, and γ ENaC subunits in the A6 apical membrane (Alvarez de la Rosa et al., 2002) is in good agreement with the time constant (18 min) for the decay in I_{Na} following administration of aprotinin. Taking changes in I_{Na} as a measure of the changes in N_T, the decrease is consistent with the retrieval of active channels from the apical membrane. This implies that aprotinin prevents a constitutive replacement of active channels while retrieval of already activated channels continues leading to an apparent turnover of uncapped channels into capped channels. If this notion is correct, aprotinin should not cause a change in cell surface protein subunit density, an expectation consistent with the biotinylation studies shown in Fig. 8. However, much higher half-life values have been reported for ENaC subunits (>24 h for α and γ, 6 h for β) in the apical membrane of A6 cells (Weisz et al., 2000; Kleyman et al., 2001). The discrep-

ancies in the measurements of ENaC subunit half-lives at the apical membrane are yet to be resolved. Since subunit half-life measurements do not necessarily correlate with the actual half-life of an active channel, we emphasize that the remarkable agreement of the estimate of the time constant for the inhibition of I_{Na} by aprotinin with the biochemical half-life observed by Alvarez de la Rosa et al. (2002) provides a working hypothesis whereby we can test the requirement of trafficking in the regulation of ENaC by endogenous proteases.

A protease-mediated uncapping that increases the N_T is at odds with recent findings that trypsin stimulates increases in "NP_o," which is equivalent to N_o (Caldwell et al., 2004). However, the increase in NP_o was only demonstrated for channels with very low NP_o resulting in 10–100-fold increases of NP_o. Inhibition by aprotinin did not reveal the presence of these 100-fold lower P_o "near-silent" channels. If these very low P_O channels were present in the absence or in the presence of aprotinin, they probably contribute a very small fraction to the total I_{Na}. If the near-silent channels are present, they do not explain the aprotinin-insensitive current and would not be detected in the presence of high P_o channels remaining in the membrane. From the perspective of transepithelial blocker–induced fluctuation analysis, the near-silent channels if present are virtually inactive. Consequently, the reduction of N_T measured here is not inconsistent with a turnover of channels with high P_o to near-silent channels in the presence of aprotinin. However, our results suggest that the higher P_o channels observed in the presence of aprotinin results either from functional heterogeneity of the Na^+ channels in the apical membrane or from compensatory increases in the P_O of active channels remaining in the membrane.

In conclusion, our data suggest there is an aprotinin-sensitive protease in the apical membrane that serves to uncap newly inserted inactive ENaC channels. It remains of interest to show whether the size of the uncapped (active) channel pool is regulated by direct proteolytic activation of apical membrane channels or via the proteolysis of coprotein(s) that in turn regulate channel activity. The possible involvement of intermediate second messengers in the protease-mediated regulation of ENaC channels will also require further investigation.

We are grateful to W. Van Driessche (K.U. Leuven, Leuven, Belgium) for providing the A6 cells.

This work was supported by National Institutes of Health grants R01-IR01DK61639 (to R. Bridges) and NRSA-F31DK015311 (to A. Adebamiro) and by the UNCF-Merck graduate research fellowship award (to A. Adebamiro).

Olaf S. Andersen served as editor.

Submitted: 11 March 2005
Accepted: 18 August 2005

REFERENCES

Abramcheck, F.J., W. Van Driessche, and S.I. Helman. 1985. Autoregulation of apical membrane Na^+ permeability of tight epithelia. Noise analysis with amiloride and CGS 4270. *J. Gen. Physiol.* 85:555–582.

Adachi, M., K. Kitamura, T. Miyoshi, T. Narikiyo, K. Iwashita, N. Shiraishi, H. Nonoguchi, and K. Tomita. 2001. Activation of epithelial sodium channels by prostasin in *Xenopus* oocytes. *J. Am. Soc. Nephrol.* 12:1114–1121.

Alvarez de la Rosa, D., H. Li, and C.M. Canessa. 2002. Effects of aldosterone on biosynthesis, traffic, and functional expression of epithelial sodium channels in A6 cells. *J. Gen. Physiol.* 119:427–442.

Alvarez de la Rosa, D., T.G. Paunescu, W.J. Els, S.I. Helman, and C.M. Canessa. 2004. Mechanisms of regulation of epithelial sodium channel by SGK1 in A6 cells. *J. Gen. Physiol.* 124:395–407.

Baxendale-Cox, L.M., R.L. Duncan, X. Liu, K. Baldwin, W.J. Els, and S.I. Helman. 1997. Steroid hormone-dependent expression of blocker-sensitive ENaCs in apical membranes of A6 epithelia. *Am. J. Physiol.* 273:C1650–C1656.

Becchetti, A., B. Malik, G. Yue, P. Duchatelle, O. Al-Khalili, T.R. Kleyman, and D.C. Eaton. 2002. Phosphatase inhibitors increase the open probability of ENaC in A6 cells. *Am. J. Physiol. Renal Physiol.* 283:F1030–F1045.

Benos, D.J., M.S. Awayda, B.K. Berdiev, A.L. Bradford, C.M. Fuller, O. Senyk, and I.I. Ismailov. 1996. Diversity and regulation of amiloride-sensitive Na^+ channels. *Kidney Int.* 49:1632–1637.

Blazer-Yost, B.L., and S.I. Helman. 1997. The amiloride-sensitive epithelial Na^+ channel: binding sites and channel densities. *Am. J. Physiol.* 272:C761–C769.

Boucher, R.C. 2004. New concepts of the pathogenesis of cystic fibrosis lung disease. *Eur. Respir. J.* 23:146–158.

Bridges, R.J., B.B. Newton, J.M. Pilewski, D.C. Devor, C.T. Poll, and R.L. Hall. 2001. Na^+ transport in normal and CF human bronchial epithelial cells is inhibited by BAY 39-9437. *Am. J. Physiol. Lung Cell. Mol. Physiol.* 281:L16–L23.

Caci, E., C. Folli, O. Zegarra-Moran, T. Ma, M.F. Springsteel, R.E. Sammelson, M.H. Nantz, M.J. Kurth, A.S. Verkman, and L.J. Galietta. 2003. CFTR activation in human bronchial epithelial cells by novel benzoflavone and benzimidazolone compounds. *Am. J. Physiol. Lung Cell. Mol. Physiol.* 285:L180–L188.

Caldwell, R.A., R.C. Boucher, and M.J. Stutts. 2004. Serine protease activation of near-silent epithelial Na^+ channels. *Am. J. Physiol. Cell Physiol.* 286:C190–C194.

Chraibi, A., and J.D. Horisberger. 2002. Na self inhibition of human epithelial Na channel: temperature dependence and effect of extracellular proteases. *J. Gen. Physiol.* 120:133–145.

Chraibi, A., V. Vallet, D. Firsov, S.K. Hess, and J.D. Horisberger. 1998. Protease modulation of the activity of the epithelial sodium channel expressed in *Xenopus* oocytes. *J. Gen. Physiol.* 111:127–138.

Danahay, H., L. Withey, C.T. Poll, S.F. van de Graaf, and R.J. Bridges. 2001. Protease-activated receptor-2-mediated inhibition of ion transport in human bronchial epithelial cells. *Am. J. Physiol. Cell Physiol.* 280:C1455–C1464.

DeFelice, L.J. 1981. Introduction to Membrane Noise. Plenum Press, New York. 257 pp.

Donaldson, S.H., A. Hirsh, D.C. Li, G. Holloway, J. Chao, R.C. Boucher, and S.E. Gabriel. 2002. Regulation of the epithelial sodium channel by serine proteases in human airways. *J. Biol. Chem.* 277:8338–8345.

Els, W.J., and S.I. Helman. 1989. Regulation of epithelial sodium channel densities by vasopressin signalling. *Cell. Signal.* 1:533–539.

Els, W.J., and S.I. Helman. 1997. Dual role of prostaglandins (PGE2) in regulation of channel density and open probability of epithelial Na^+ channels in frog skin (*R. pipiens*). *J. Membr. Biol.* 155:75–87.

Els, W.J., S.I. Helman, and T. Mencio. 1991. Activation of epithelial Na channels by hormonal and autoregulatory mechanisms of action. *J. Gen. Physiol.* 98:1197–1220.

Garty, H. 2000. Regulation of the epithelial Na^+ channel by aldosterone: open questions and emerging answers. *Kidney Int.* 57: 1270–1276.

Garty, H., and L.G. Palmer. 1997. Epithelial sodium channels: function, structure, and regulation. *Physiol. Rev.* 77:359–396.

Gottardi, C.J., L.A. Dunbar, and M.J. Caplan. 1995. Biotinylation and assessment of membrane polarity: caveats and methodological concerns. *Am. J. Physiol.* 268:F285–F295.

Granitzer, M., T. Leal, W. Nagel, and J. Crabbe. 1991. Apical and basolateral conductance in cultured A6 cells. *Pflugers Arch.* 417: 463–468.

Granitzer, M., W. Nagel, and J. Crabbe. 1992. Basolateral membrane conductance in A6 cells: effect of high sodium transport rate. *Pflugers Arch.* 420:559–565.

Hanwell, D., T. Ishikawa, R. Saleki, and D. Rotin. 2002. Trafficking and cell surface stability of the epithelial Na^+ channel expressed in epithelial Madin-Darby canine kidney cells. *J. Biol. Chem.* 277: 9772–9779.

Helman, S.I., and L.M. Baxendale. 1990. Blocker-related changes of channel density. Analysis of a three-state model for apical Na channels of frog skin. *J. Gen. Physiol.* 95:647–678.

Helman, S.I., and N.L. Kizer. 1990. Apical Sodium Ion Channels of Tight Epithelia as Viewed from the Perspective of Noise Analysis. Vol. 37. Academic Press, San Diego. 117–155.

Helman, S.I., and X. Liu. 1997. Substrate-dependent expression of Na^+ transport and shunt conductance in A6 epithelia. *Am. J. Physiol.* 273:C434–C441.

Helman, S.I., X. Liu, K. Baldwin, B.L. Blazer-Yost, and W.J. Els. 1998. Time-dependent stimulation by aldosterone of blocker-sensitive ENaCs in A6 epithelia. *Am. J. Physiol.* 274:C947–C957.

Hughey, R.P., J.B. Bruns, C.L. Kinlough, K.L. Harkleroad, Q. Tong, M.D. Carattino, J.P. Johnson, J.D. Stockand, and T.R. Kleyman. 2004. Epithelial sodium channels are activated by furin-dependent proteolysis. *J. Biol. Chem.* 279:18111–18114.

Hughey, R.P., G.M. Mueller, J.B. Bruns, C.L. Kinlough, P.A. Poland, K.L. Harkleroad, M.D. Carattino, and T.R. Kleyman. 2003. Maturation of the epithelial Na^+ channel involves proteolytic processing of the α- and γ-subunits. *J. Biol. Chem.* 278:37073–37082.

Jovov, B., N.K. Wills, P.J. Donaldson, and S.A. Lewis. 1990. Vectorial secretion of a kallikrein-like enzyme by cultured renal cells. I. General properties. *Am. J. Physiol.* 259:C869–C882.

Kleyman, T.R., J.B. Zuckerman, P. Middleton, K.A. McNulty, B. Hu, X. Su, B. An, D.C. Eaton, and P.R. Smith. 2001. Cell surface expression and turnover of the α-subunit of the epithelial sodium channel. *Am. J. Physiol. Renal Physiol.* 281:F213–F221.

Kunzelmann, K., R. Schreiber, and A. Boucherot. 2001. Mechanisms of the inhibition of epithelial Na^+ channels by CFTR and purinergic stimulation. *Kidney Int.* 60:455–461.

Li, J.H., and B. Lindemann. 1983. Competitive blocking of epithelial sodium channels by organic cations: the relationship between macroscopic and microscopic inhibition constants. *J. Membr. Biol.* 76:235–251.

Li, J.H., L.G. Palmer, I.S. Edelman, and B. Lindemann. 1982. The role of sodium-channel density in the natriferic response of the toad urinary bladder to an antidiuretic hormone. *J. Membr. Biol.* 64:77–89.

Lindemann, B., and W. Van Driessche. 1978. The mechanism of Na uptake through Na-selective channels in the epithelium of frog skin. *Membrane Transport Processes.* 1:155–179.

Liu, L., K.S. Hering-Smith, F.R. Schiro, and L.L. Hamm. 2002. Serine protease activity in m-1 cortical collecting duct cells. *Hypertension.* 39:860–864.

Margolius, H.S., and J. Chao. 1980. Amiloride inhibits mammalian renal kallikrein and a kallikrein-like enzyme from toad bladder and skin. *J. Clin. Invest.* 65:1343–1350.

Masilamani, S., G.H. Kim, C. Mitchell, J.B. Wade, and M.A. Knepper. 1999. Aldosterone-mediated regulation of ENaC α, β, and γ subunit proteins in rat kidney. *J. Clin. Invest.* 104:R19–R23.

Nadal, M.S., A. Ozaita, Y. Amarillo, E. Vega-Saenz de Miera, Y. Ma, W. Mo, E.M. Goldberg, Y. Misumi, Y. Ikehara, T.A. Neubert, and B. Rudy. 2003. The CD26-related dipeptidyl aminopeptidase-like protein DPPX is a critical component of neuronal A-type K^+ channels. *Neuron.* 37:449–461.

Nakhoul, N.L., K.S. Hering-Smith, C.T. Gambala, and L.L. Hamm. 1998. Regulation of sodium transport in M-1 cells. *Am. J. Physiol.* 275:F998–F1007.

Narikiyo, T., K. Kitamura, M. Adachi, T. Miyoshi, K. Iwashita, N. Shiraishi, H. Nonoguchi, L.M. Chen, K.X. Chai, J. Chao, and K. Tomita. 2002. Regulation of prostasin by aldosterone in the kidney. *J. Clin. Invest.* 109:401–408.

Orce, G.G., G.A. Castillo, and H.S. Margolius. 1980. Inhibition of short-circuit current in toad urinary bladder by inhibitors of glandular kallikrein. *Am. J. Physiol.* 239:F459–F465.

Palmer, L.G. 1992. Epithelial Na channels: function and diversity. *Annu. Rev. Physiol.* 54:51–66.

Palmer, L.G., and G. Frindt. 1988. Conductance and gating of epithelial Na channels from rat cortical collecting tubule. Effects of luminal Na and Li. *J. Gen. Physiol.* 92:121–138.

Palmer, L.G., and G. Frindt. 1996. Gating of Na channels in the rat cortical collecting tubule: effects of voltage and membrane stretch. *J. Gen. Physiol.* 107:35–45.

Paunescu, T.G., B.L. Blazer-Yost, C.J. Vlahos, and S.I. Helman. 2000. LY-294002-inhibitable PI 3-kinase and regulation of baseline rates of Na^+ transport in A6 epithelia. *Am. J. Physiol. Cell Physiol.* 279:C236–C247.

Planes, C., C. Leyvraz, T. Uchida, M.A. Angelova, G. Vuagniaux, E. Hummler, M.A. Matthay, C. Clerici, and B.C. Rossier. 2005. In vitro and in vivo regulation of transepithelial lung alveolar sodium transport by serine proteases. *Am J Physiol Lung Cell Mol Physiol.* 288:L1099–L1109.

Puoti, A., A. May, C.M. Canessa, J.D. Horisberger, L. Schild, and B.C. Rossier. 1995. The highly selective low-conductance epithelial Na channel of *Xenopus laevis* A6 kidney cells. *Am. J. Physiol.* 269:C188–C197.

Rokaw, M.D., D.J. Benos, P.M. Palevsky, S.A. Cunningham, M.E. West, and J.P. Johnson. 1996. Regulation of a sodium channel-associated G-protein by aldosterone. *J. Biol. Chem.* 271:4491–4496.

Rossier, B.C. 2004. The epithelial sodium channel: activation by membrane-bound serine proteases. *Proc. Am. Thorac. Soc.* 1:4–9.

Shipway, A., H. Danahay, J.A. Williams, D.C. Tully, B.J. Backes, and J.L. Harris. 2004. Biochemical characterization of prostasin, a channel activating protease. *Biochem. Biophys. Res. Commun.* 324: 953–963.

Snyder, P.M. 2000. Liddle's syndrome mutations disrupt cAMP-mediated translocation of the epithelial Na^+ channel to the cell surface. *J. Clin. Invest.* 105:45–53.

Snyder, P.M. 2002. The epithelial Na^+ channel: cell surface insertion and retrieval in Na^+ homeostasis and hypertension. *Endocr. Rev.* 23:258–275.

Snyder, P.M., D.B. Bucher, and D.R. Olson. 2000. Gating induces a

conformational change in the outer vestibule of ENaC. *J. Gen. Physiol.* 116:781–790.

Tang, J., F.J. Abramcheck, W. Van Driessche, and S.I. Helman. 1985. Electrophysiology and noise analysis of K^+-depolarized epithelia of frog skin. *Am. J. Physiol.* 249:C421–C429.

Tong, Z., B. Illek, V.J. Bhagwandin, G.M. Verghese, and G.H. Caughey. 2004. Prostasin, a membrane-anchored serine peptidase, regulates sodium currents in JME/CF15 cells, a cystic fibrosis airway epithelial cell line. *Am. J. Physiol. Lung Cell. Mol. Physiol.* 287:L928–L935.

Vallet, V., A. Chraibi, H.P. Gaeggeler, J.D. Horisberger, and B.C. Rossier. 1997. An epithelial serine protease activates the amiloride-sensitive sodium channel. *Nature.* 389:607–610.

Vallet, V., C. Pfister, J. Loffing, and B.C. Rossier. 2002. Cell-surface expression of the channel activating protease xCAP-1 is required for activation of ENaC in the *Xenopus* oocyte. *J. Am. Soc. Nephrol.* 13:588–594.

Van Driessche, W., and B. Lindemann. 1978. Low-noise amplification of voltage and current fluctuations arising in epithelia. *Rev. Sci. Instrum.* 49:53–57.

Van Driessche, W., and B. Lindemann. 1979. Concentration dependence of currents through single sodium-selective pores in frog skin. *Nature.* 282:519–520.

Vogel, R., and E. Werle. 1970. Handbook of Experimental Pharmacology. Bradykinin, Kallidin, and Kallikrein. Vol. 25. Springer, Berlin. 213–249.

Vuagniaux, G., V. Vallet, N.F. Jaeger, E. Hummler, and B.C. Rossier. 2002. Synergistic activation of ENaC by three membrane-bound channel-activating serine proteases (mCAP1, mCAP2, and mCAP3) and serum- and glucocorticoid-regulated kinase (Sgk1) in *Xenopus* oocytes. *J. Gen. Physiol.* 120:191–201.

Vuagniaux, G., V. Vallet, N.F. Jaeger, C. Pfister, M. Bens, N. Farman, N. Courtois-Coutry, A. Vandewalle, B.C. Rossier, and E. Hummler. 2000. Activation of the amiloride-sensitive epithelial sodium channel by the serine protease mCAP1 expressed in a mouse cortical collecting duct cell line. *J. Am. Soc. Nephrol.* 11: 828–834.

Weisz, O.A., J.M. Wang, R.S. Edinger, and J.P. Johnson. 2000. Non-coordinate regulation of endogenous epithelial sodium channel (ENaC) subunit expression at the apical membrane of A6 cells in response to various transporting conditions. *J. Biol. Chem.* 275: 39886–39893.